FISEVIER

Contents lists available at ScienceDirect

# Science of the Total Environment

journal homepage: www.elsevier.com/locate/scitotenv



# Plasma-enhanced electrostatic precipitation of diesel exhaust particulates using nanosecond high voltage pulse discharge for mobile source emission control



Boxin Zhang <sup>b,1</sup>, Indu Aravind <sup>a,1</sup>, Sisi Yang <sup>a</sup>, Sizhe Weng <sup>c</sup>, Bofan Zhao <sup>c</sup>, Christi Schroeder <sup>a</sup>, William Schroeder <sup>a</sup>, Mark Thomas <sup>d</sup>, Ryan Umstattd <sup>d</sup>, Dan Singleton <sup>d</sup>, Jason Sanders <sup>d</sup>, Heejung Jung <sup>e,f</sup>, Stephen B. Cronin <sup>a,b,c,\*</sup>

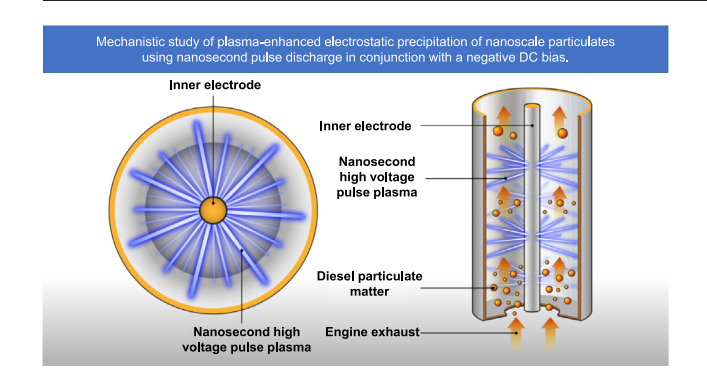
- <sup>a</sup> Department of Physics and Astronomy, University of Southern California, Los Angeles, CA 90089, USA
- b Mork Family Department of Chemical Engineering and Materials Science, University of Southern California, Los Angeles, CA 90089, USA
- <sup>c</sup> Ming Hsieh Department of Electrical Engineering, University of Southern California, Los Angeles, CA 90089, USA
- <sup>d</sup> Transient Plasma Systems, Inc., Torrance, CA 90501, USA
- <sup>e</sup> Department of Mechanical Engineering, University of California, Riverside, Riverside, CA 92507, USA
- f College of Engineering-Center for Environmental Research and Technology (CE-CERT), University of California, Riverside, Riverside, CA 92507, USA

#### HIGHLIGHTS

# PE-ESP demonstrates 95% remediation of PM and consumes less than 1% of the engine power

- Plasma enhancement enables high remediation at low DC voltages and smaller reactors
- Numerical simulations verify the chargebased mechanism of enhancement provided by the nanosecond high voltage pulse plasma

#### GRAPHICAL ABSTRACT



# ARTICLE INFO

Editor: Pavlos Kassomenos

Keywords:
Pollution control
Particulate matter
PM
Soot
PE-ESP
Exhaust

# ABSTRACT

This study reports enhancement in the electrostatic precipitation (ESP) of diesel engine exhaust particulates using high voltage nanosecond pulse discharge in conjunction with a negative direct current (DC) bias voltage. The high voltage (20 kV) nanosecond pulses produce ion densities that are several orders of magnitude higher than those in the corona produced by a standard DC-only ESP. This plasma-enhanced electrostatic precipitator (PE-ESP) demonstrated 95 % remediation of PM and consumes less than 1 % of the engine power (i.e., 37 kW diesel engine at 75 % load). While the DC-only ESP remediation increases linearly with applied voltage, the plasma-enhanced ESP remains approximately constant over the applied range of negative DC biases. Numerical simulations of the PE-ESP process agree with the DC-only experimental results and enable us to verify the charge-based mechanism of enhancement provided by the nanosecond high voltage pulse plasma. Two different reactor configurations with different flow rates yielded the same remediation values despite one having half the flow rate of the other. This indicates that the reactor can be made even smaller without sacrificing performance. Here, this study finds that the plasma enhancement enables high remediation values at low DC voltages and smaller ESP reactors to be made with high remediation.

<sup>\*</sup> Corresponding author at: Department of Electrical Engineering, University of Southern California, Los Angeles, CA 90089, USA. *E-mail address*: scronin@usc.edu (S.B. Cronin).

Authors contributed equally.

## 1. Introduction

During the past decades, the adverse health effects of diesel particulate emissions have been firmly established by many toxicological studies (Lighty et al., 2000; Burtscher, 2005; Brown et al., 2001; Oberdörster et al., 2004). In epidemiological studies, fine particulates (particles smaller than 2.5 µm) have been linked to premature cardiovascular and respiratory deaths in metropolitan areas, as well as lung cancer (Samet et al., 2000; Pope et al., 2002; Chow et al., 2006; Oberdörster et al., 2005; Dockery et al., 1993). In 2012, the International Agency for Research on Cancer (IARC), which is part of the World Health Organization (WHO), declared diesel exhaust as carcinogenic to humans (IARC, 2012; Panel, 2015; Ristovski et al., 2012; Ris, 2007). Several technological approaches have been developed to mitigate diesel particulates, including diesel particulate filters (DPFs), and electrostatic precipitators (ESP) (Schauer et al., 1999; Saiyasitpanich et al., 2007; Sudrajad and Yusof, 2015). Many of these have been developed in response to increasingly stringent air quality regulations. While engine-powered light duty vehicles are expected to be replaced with battery-powered electric vehicles with the current popular trend towards zero-emissions systems, for most practical applications which demand high power such as ships, trucks, and backup generators, diesel engines will remain a dominant source of power, requiring more advanced pollution control devices to be developed. Diesel particulate filters are successful in mitigating emissions from light-duty and heavy-duty vehicles, but they are not easily scalable to large engines such as ship engines.

Remediation of diesel exhaust via electrostatic precipitation (ESP) has been studied by many research groups over the past four decades. However, this approach suffers from large reactor size requirements and, thus, is not suitable for mobile sources for ground transportation (Kittelson et al., 1986). The large footprint of ESPs is less of concern on large ships, however, it is clear that downsizing can lower the cost for both installation and operation. It is also worth noting that, using electrostatic precipitation, carbon is captured not oxidized, thus, reducing  $\rm CO_2$  emissions. For example, commonly used diesel particulate filters (DPFs) are regenerated through an oxidation procedure that ultimately converts the carbonaceous PM to  $\rm CO_2$ , releasing global warming gases into the atmosphere. When DPFs are applied without regeneration, the filter becomes clogged resulting in severe backpressure on the engine, lower engine efficiencies, increased GHG emissions, and eventually stalling of the engine.

There have been several studies using conventional (DC only) electrostatic precipitators (i.e., without pulsed plasma) to treat diesel PM (Kim et al., 2015; Kim et al., 2013). In DC-only ESPs, the DC voltage is responsible for charging the nanoscale particulates (via corona discharge) and sweeping them to the sidewalls of the reactor. Many of these studies entailed small laboratory-scale reactors to treat a partial fraction of the engine exhaust (Hayashi et al., 2009; Takasaki et al., 2015; Zukeran et al., 2019). In studies using conventional ESPs to treat full engine exhaust, the typical range of voltages were between 7 and 70 kV, resulting in remediation efficacies ranging from 70 to 80 % (Saiyasitpanich et al., 2007; Silvestre de Ferron et al., 2008; Hayashi, 2011). Here, remediation efficacies are obtained by filter-based measurements and defined as (particle mass with remediation - particle mass without remediation)/(particle mass without remediation). In one study, a wet electrostatic precipitator using a DC voltage was used to treat diesel PM with efficacies in this range, however, only at 0 % engine load (i.e., idle) (Saiyasitpanich et al., 2007). Zukeran et al. used a two-stage ESP to achieve 78 % remediation of diesel PM after allowing the exhaust to cool down to room temperature with a heat exchanger (Zukeran and Ninomiya, 2013). Crespo et al. achieved remediation efficiencies above 85 % with a conventional DConly ESP using a similar approach of allowing the exhaust gas to cool to room temperature. It is important to note that arcing threshold voltages are significantly higher at room temperature, which is advantageous for electrostatic precipitation. However, the general methodology of allowing the exhaust gas to cool to room temperature does not represent a feasible approach for practical applications. At high enough DC voltages, dielectric breakdown occurs resulting in the formation of a highly conducting arc (see

Fig. S1), which collapses the electrostatic field between the two electrodes terminating the electrostatic precipitation process. Nanosecond high voltage pulses provide a way around this arcing threshold, enabling substantially higher peak fields to be achieved without arcing.

Nonthermal plasmas (e.g., pulsed voltage dielectric barrier discharge) have been used to treat diesel emissions reporting reductions in both NOx and diesel particulate matter (DPM) by several research groups (Vinh et al., 2012; Fushimi et al., 2008; Kuwahara et al., 2020; Okubo et al., 2017; Song et al., 2009; Okubo et al., 2010). Non-thermal plasmas created using high voltage nanosecond pulses consume far less energy in the creation of the plasma than conventional radio frequency (RF) sources. The transient nature of the plasma necessitates that very little current is drawn in creating the plasma. That is, once the streamer is created, the applied field collapses before a substantial amount of current (and hence electric power) can flow. Because of its transient nature, this is a cold plasma, in which the electron energies are around 30 eV, while the vibrational modes of the molecules remain at room temperature (i.e., out of thermal equilibrium). These "hot" electrons enable higher ion densities to be achieved in the plasma through the formation of energetic intermediate species that are otherwise not possible via corona discharge. Previous studies using nonthermal plasma were typically carried out on small lab-scale reactors that treat only a fraction of the engine exhaust (i.e., slipstream configuration) rather than the full engine exhaust flow. Remediation efficiencies on the order of 1 g/kWh are typically reported (Fushimi et al., 2008; Okubo et al., 2010). If we consider the 37 kW diesel engine in our present study, an electrical power of 3.2 kW would be needed in order to remediate 95 % of the DPM. This corresponds to 9 % of the engine power and, thus, does not represent a feasible approach for practical applications.

While microsecond high voltage pulses have been utilized to enhance electrostatic precipitators (Silvestre de Ferron et al., 2008; Won-Ho et al., 1999; Grass et al., 2001; Hall, 1990), the use of nanosecond high voltage pulses (i.e., peak voltages above 10 kV and pulse durations less than 50 ns, see Fig. 1d) has not been reported to enhance the treatment of diesel exhaust via ESP. (Bidoggia et al., 2020; Grass et al., 2004) There are several important differences between µsec and nsec high voltage pulses in regards to ESP functionality, the first of which is power efficiency. Since the energy per pulse increases with pulse duration, nanosecond pulses are approximately 1000 × more efficient than µsec pulses at the same peak voltage (see Fig. S1). For a nsec pulse, once the streamer is formed, the electric field drops to zero before a substantial amount of current can flow and power can be dissipated. More importantly, the fast rise times of these nsec pulses (that is,  $dV/dt \sim 10^{12} \text{ V/s}$ ) produce a streamer discharge, as depicted in Fig. 1e. This streamer discharge has a significantly higher  $(\sim 10^6 \times)$  ion concentration than those in the corona discharge generated by constant DC bias voltages in conventional ESPs. Here, it is important to note that it is actually the pulse rise time (i.e., dV/dt), rather than pulse duration, that determines the streamer density, which includes both the ion concentration within each streamer and the number of streamers per length of electrode wire (Winands et al., 2008; Teunissen et al., 2014; Babaeva and Naidis, 2016; Huiskamp et al., 2017). A corona discharge, which is localized to the electrode surface, is fundamentally different from streamer discharge, which extends further away from the electrode surface, as illustrated in Fig. S1 of the Supplemental Document. The increased charge densities associated with streamer discharge, especially away from the electrode surfaces, are particularly advantageous for ESP remediation and ultimately enable more compact ESPs to be designed. As compared to corona discharge, this streamer discharge produces extremely high peak ion densities that can ultimately enable more compact ESPs to be designed. In the high temperature diesel exhaust environment, arcing threshold voltages are considerably lower, and the charged radical species in the plasma have shorter lifetimes. The nsec high voltage pulses provide a way around this limitation enabling both higher peak fields and higher ion densities to be achieved.

This study investigates the effect of transient plasma on the electrostatic precipitation of diesel particulates under engine-relevant conditions. The DC voltage is swept over a wide range while particle

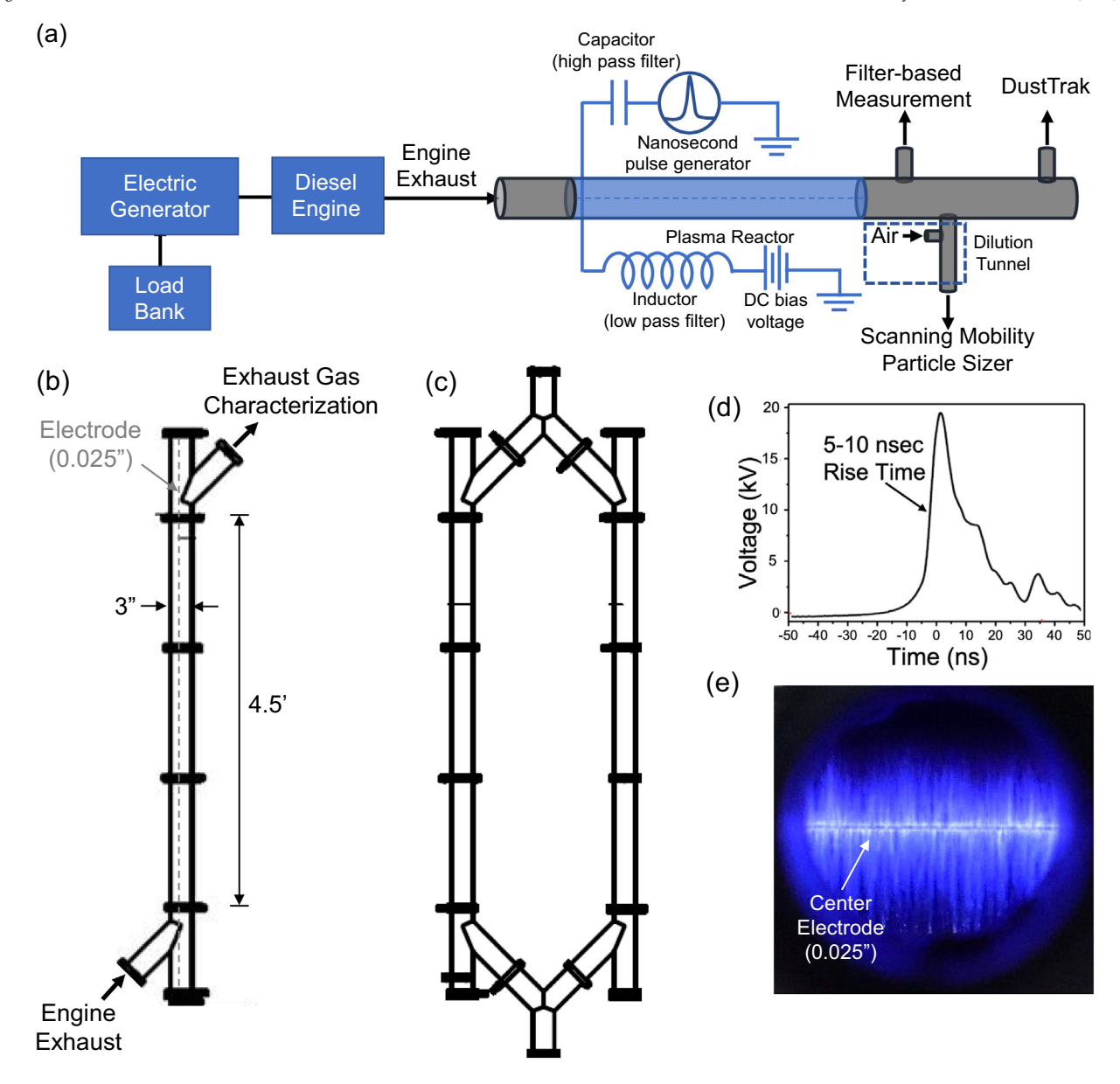


Fig. 1. (a) Schematic diagram of the measurement setup used for characterizing the plasma-enhanced electrostatic precipitator (PE-ESP) system. Design diagram of the (a) single and (b) double PE-ESP reactors. (d) Typical output characteristics of the nanosecond high voltage pulse generator. (e) Photograph of the transient plasma formed by high voltage nanosecond pulse discharge.

emissions are measured with and without the plasma. Three techniques were used to measure these particle emissions (filter-based measurement, optical detection, and mobility particle sizer measurements), to provide additional perspective on the remediation mechanism. Different reactor geometries were compared in order to evaluate how the remediation efficiency depends on residence time, i.e., how long each volumetric element spends in the reactor (t= reactor volume/volumetric flow rate). Numerical simulations of the electrostatic precipitation were performed to provide a microscopic understanding of the complex remediation process and identify the key limiting factors, sources of loss and inefficiencies.

# 2. Materials and methods

Fig. 1 shows a schematic diagram of the experimental approach. A 37 kW (49 HP) diesel generator is attached to an electric generator (Generac Model SD030, emission level: Tier 4, rated RPM: 1800) and resistive load bank (Avtron Model LPH75 Liberty D42034) run at 75 % engine

load in steady state. The full exhaust from the engine is then flowed through a 3"-diameter, 4.5'-long coaxial stainless-steel reactor with a 0.025"-diameter center wire, as illustrated in Fig. 1b. Fig. 1c shows an alternate reactor geometry in which two coaxial reactors are configured in parallel, thus, doubling the reactor volume and residence time (from 0.54~s to 0.96~s) at a given exhaust flow rate. The transient pulsed plasma is produced with a high voltage nanosecond pulse generator (Model SSPG-20X, Transient Pulsed System, Inc.), which produces pulses with peak voltages up to 20 kV, pulse rise times of 5–10 ns, and repetition rates of 1 kHz. A typical waveform is shown in Fig. 1d. Fig. 1a shows a circuit diagram illustrating how the nanosecond pulse generator is configured together with the high voltage DC power supply ( $V_{DC} = -10$  to -17 kV). Here, a capacitor (high pass filter) protects the nanosecond pulse generator from the applied DC high voltages (V<sub>DC</sub>), and the inductor (low pass filter) protects the DC high voltage power supply from the high voltage nanosecond pulses  $(V_{nsec} = +20 \text{ kV})$  (Yang et al., 2021a; Yang et al., 2021b). These voltages (V<sub>nsec</sub> and V<sub>DC</sub>) are added together on the center wire of the reactor, while the outer cylinder is kept at electrical ground.

Diesel particle concentrations were measured using three separate methods: filter-based gravimetric measurements, online measurement with scanning mobility particle sizer (SMPS Model 308,200, TSI Inc.) and DustTrak (Model 8530, TSI Inc.) with and without the nanosecond pulsed plasma. The filter-based gravimetric measurements were carried out by a third-party testing facility Olson-Ecologic Engine Testing Laboratory (Fullerton, CA), which is an EPA and CARB-recognized engine testing facility. These tests follow the protocol from a Code of Federal Regulation (CFR) 1065, as defined by the U.S. EPA to measure PM2.5 mass of the exhaust particles collected on a filter medium (Code of Federal Regulations (CFR) Title 40 - Protection of Environment, 2022). In these measurements, the filters are weighed before and after flowing a controlled amount of engine exhaust through the filters using an AVL advanced dilution system (AVL SPC 472). For the latter two methods, a dilution tunnel was used to dilute the diesel exhaust with a dilution ratio of 7.9 with room-temperature compressed dry air (Grade 0) before feeding them to the SMPS and DustTrak, as illustrated in Fig. 1a. This dilution ratio was determined by measuring the CO<sub>2</sub> concentrations before and after dilution using a Horiba portable gas analyzer. The primary goal of dilution is to quench further changes in the physical and chemical properties of the particles and exhaust gas. As such it has a cooling effect and a dilution effect. The cooling effect increases the supersaturation ratio, while the dilution effect lowers the supersaturation ratio for nucleation mode generation. We have not observed any nucleation mode in our study, and the dilution ratio used here is typical for these applications. Using this configuration, the exhaust gas temperature was 184 °C (double reactor) and 225 °C (single reactor), the volumetric flow rate was 773 lpm (double reactor) and 697 lpm (single reactor), linear flow rates determined based on the volumetric flow rates and the cross sectional areas of the reactors were 1.42 m/s (double reactor) and 2.56 m/s (single reactor), residence times were 0.96 s (double reactor) and 0.54 s (single reactor), and the humidity was 16.2 %. The reason that the double reactor has slightly higher volume flow rate is likely due to lower exhaust temperature at the double reactor. Note mass exhaust flow rate needs to be conserved i.e., volumetric flow times density of the exhaust flow should be constant.

The DustTrak responds to a photometric signal from aerosol streams at a 90-degree scattering angle from the incident laser illumination. Its USER manual specifies that the instrument responds from approximately 0.1 to 10  $\mu m$  particle size range. However, it is known that detection of diesel particles scattering below 0.3  $\mu m$  is extremely challenging and often negligible. The DustTrak reports aerosol mass concentration in  $mg/m^3$ , and the light scattering signal is calibrated against filter measured mass concentrations of the test aerosol for this conversion. The default is based on the calibration using Arizona test dust (ISO 12103-1, A1) (Khan et al., 2012). As different calibration aerosols determine different calibration factors, which are one-point calibrations, they only change the calibration slope (Khan et al., 2012; Moosmüller et al., 2001; Jamriska et al., 2004). Despite the DustTrak's limitations in ultra-fine particle detection, when taken together in conjunction with the SMPS and filter-based measurements, they provide additional insight into the PM remediation process.

The SMPS measures particle size distributions based on their electrical mobility diameters. Total particle numbers are obtained by integrating particle number for each size distribution, and this was used to determine remediation based on SMPS measurements. It should be noted that while the gravimetric filter method and DustTrak determined remediation based on particle mass, the SMPS determined remediation based on particle number. Since the mean or median diameters of diesel exhaust particles are different for mass and number metrics, it is expected that the remediation value may be dependent on particle metric and size range the instrument has measured. In the Results and discussion section, number mean and mass mean diameter of the diesel particles will be discussed along with the remediation percentage.

Regulations of diesel particles are based on gravimetrically measured particle mass. While these are regulatorily relevant, they do not provide any insight into the mechanism of remediation, such as size dependence. The SMPS measurements, on the other hand, determine the particle size

distribution, which provides insight on remediation based on the particle number concentrations. The DustTrak is a convenient screening device widely used among researchers and, as such, we have provided the data along with remediation by particle mass and number. While the SMPS is limited to sub-micron size particles, the DustTrak can detect particles up to  $10\ \mu m$  in size.

#### 3. Results and discussion

The application of both positive and negative DC bias voltages is possible using this PE-ESP setup. However, we have found that higher DC bias voltages can be achieved with negative bias than with positive bias. As such negative DC bias voltages were found to produce higher remediation of DPM than positive DC voltages. For example, the highest positive voltage we could achieve was +10 kV. This resulted in half the remediation that we achieved with -14.5 kV. This is somewhat surprising since positive DC voltages and positive nsec pulse voltages sum additively, while negative DC voltages and positive pulses sum destructively. The benefit of negative DC biases over positive DC biases arises mainly because the arcing threshold is lower for positive DC voltages than for negative DC voltages. The sharp curvature around the center wire electrode (i.e., 0.025") produces a significant amount of electric field enhancement, while the outer cylindrical electrode has no field enhancement. Arcing is usually initiated by the field emission of electrons from the metal surface at high electric fields. When the center wire electrode is configured as the cathode (i.e., electron emitter) under positive bias, this field enhancement leads to lower arcing thresholds, which is disadvantageous for ESP. However, when the center wire electrode is configured as the anode (i.e., negative bias), the field enhancement does not lead to significant reduction in arcing thresholds. This work focuses on the result using negative DC bias voltage, and the result using positive DC bias voltage will be investigated in a following study.

Fig. 2 shows a comparison of the remediation values (in percent) of the diesel particulate matter (DPM) measured with and without high voltage nanosecond pulses (  $\pm$  20 kV peak voltage, at a repetition rate of 1 kHz) plotted as a function of DC bias voltage from  $\pm$  10 kV to  $\pm$  17 kV. Fig. 2a–c show remediation values taken with the three different characterization methods described above. Here, the dashed lines represent data taken with a single reactor (drawn in Fig. 1b), and the solid lines represent data taken with two reactors in parallel (i.e., "double reactor"), as illustrated in Fig. 1c. In these plots, the open symbols correspond to data taken with DC voltage only, and the filled symbols correspond to DC voltage plus nsec pulses. Based on these three datasets, we make the following observations.

The single reactor performs just as well as the double reactor, despite the fact that it has twice the linear flow velocity (and half the reactor volume) as that of the double reactor. This means that this single reactor can likely treat even higher flow rates with the same performance, and/or this reactor can be made even shorter (smaller) without sacrificing performance. This also means the remediation in the single reactor is not limited by charging or migration time of the particle suggesting the single reactor can be further reduced in length. In addition, the remediation values measured with the filter-based method are approximately 10 % lower than those of the SMPS and DustTrak. Since the response of the DustTrak is calibrated against gravimetrically measured particle mass concentrations, one would expect the remediation values determined by filter-based measurements to agree with that of the DustTrak. We speculate that the higher remediation values obtained by the DustTrak (compared to SMPS) to arise from the uncertainties between gravimetric and photometric methods. In these datasets, the highest remediation value was 95 %, as measured by the SMPS (or by total number) and is higher than previous reports.

The enhancement produced by the high voltage nanosecond pulses is more pronounced at smaller (absolute value) DC bias voltages (i.e.,  $-10 \, \text{kV}$ ) than at larger DC biases (i.e.,  $-17 \, \text{kV}$ ). The use of lower DC voltages is advantageous for avoiding arcing and providing more stable operation particularly under the rapidly changing exhaust conditions (e.g., temperature, humidity, etc.) of mobile sources. More specifically,

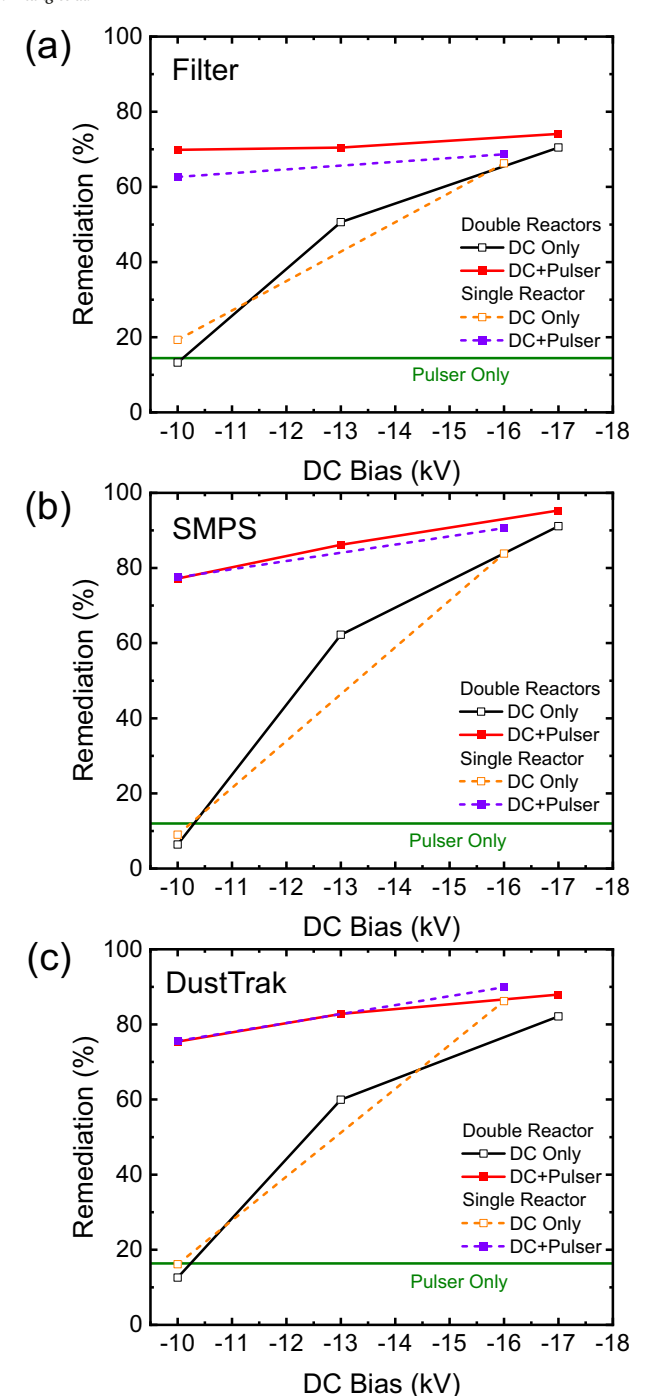


**Fig. 2.** Diesel particulate matter (DPM) remediation (%) for nanosecond high voltage pulses (20 kV at 1 kHz) plotted as a function of the applied DC bias voltage for single and double (in parallel) reactors. Plots show data taken with (a) filter-based method (ISO 8178), (b) scanning mobility particle sizer with a charge particle counter, and (c) optical based detection (i.e., DustTrak).

we observe a 12× enhancement in the remediation % at  $V_{\rm DC}=-10~kV$  and just 1.05× at  $V_{\rm DC}=-17~kV$ , as measured by SMPS. The data at  $V_{\rm DC}=-17~kV$  produces nearly the same remediation with and without the high voltage nanosecond pulses. However, it should be noted that this voltage is unstable with many arcing events occurring over the duration of the measurement, and we cannot apply DC voltages below  $V_{\rm DC}=-17~kV$  because of arcing. At  $V_{\rm DC}=-17~kV$ , the ion density produced by the corona is relatively high ( $\sim 10^9~cm^{-3}$ ). As such, the additional benefit of introducing the transient plasma is negligible. This means that,

at  $V_{\rm DC}=-17$  kV, the charging of nanoparticles is not a limiting step in the ESP process. However, above  $V_{\rm DC}<-17$  kV, the charging of nanoparticles is a limiting factor in the overall efficacy of the ESP process. A qualitative comparison of the SMPS data taken under various pulser and DC bias conditions is plotted in Fig. S2 of the SI document, and no significant shift in the particle size distribution is observed.

Data taken with the pulser only (i.e., no DC bias) produces only 12–16 % remediation. 14.5 % remediation, as measured by filter-based measurements, 12 %, as measured by SMPS, and 16.4 % as measured by DustTrak. The double reactor enabled higher DC voltages to be applied without arcing, since the double reactor has a cooler exhaust temperature due to the larger reactor surface area for heat transfer. It is possible that the plasma could generate nanoparticles by sputtering/ablating material off the center electrode, as reported by Mun et al. (i.e., plasma jet process) (Turan et al., 2021; Kim and Kim, 2019; Mun et al., 2020). However, we believe that this effect is negligible compared to the electrostatic precipitation process. We have performed pulser-only measurements without a DC bias (horizontal green lines in Fig. 2). This data exhibits a remediation of 12–16 %. If there was significant nanoparticle generation, then the remediation would be negative (i.e., no remediation).

In order to obtain a better understanding of the PE-ESP process, we have performed numerical simulations using the multi-physics COMSOL package (Lawless and Sparks, 1988; The Plasma Module User's Guide, n.d.; Particle Tracing Module User's Guide, n.d.; Lawless and Altman, 1994; Wang et al., 2019; Rubinetti et al., 2015). This model is based on a five step multi-physics calculation, which includes the following: 1. Plasma Chemistry (Ionization) Model, 2. Electrostatic Poison's Equation, 3. Navier-Stokes Equation, 4. Particle Charging Model, 5. Remediation % vs. Particle Diameter. In these simulations, the connection between fluid dynamics and electrostatics is established through the forces exerted on the charged particles, namely drag forces and Coulomb forces. The physical model for the fluid dynamics part is based on incompressible Navier-Stokes equations. The resulting velocity field is used in the drag model for particle motion. For sub-micron diameter particles, the drag forces are corrected by the Cunningham slip correction factor, which bridges the gap between the molecular and continuum regimes. The second major force acting on particles is the Coulomb force, which is the product of particle charge and the surrounding electric field. The ionization by plasma discharge is currently described by coupling Poisson's equation with the continuity equation for space charge density. The corresponding boundary condition for the emitting electrode relates the electric field to the space charge density. A time domain simulation is carried out to determine the instantaneous charge and trajectory of particles. In the beginning, electrically neutral particles of varying diameters are uniformly distributed along the radial direction at the bottom of the reaction chamber. This treatment assumes that overwhelmingly higher ion concentrations will wipe out any pre-existing charge effects on the soot. The charge accumulated on particles as they flow through a region of high electric field and space charge density is modelled using the Lawless model. The trajectories of particles are calculated by considering the net force acting on the particles at each instant. The net charge on each particle becomes stabilized over time. The average charge on particles is calculated considering the net charge on particles at the end of the simulation.

Fig. 3a shows a schematic diagram of the electrostatic precipitation process for a coaxial cylindrical reactor geometry. As part of Steps 1 and 2 in this simulation, we calculate the radial ion distributions within the electrostatic precipitator reactor. Fig. 3b shows the calculated remediation percentage plotted as a function of the applied (negative) DC voltage for 100 nm diameter nanoparticles. Note, this calculation is for DC only meaning unipolar charging condition with no nanosecond high voltage pulses. The DC voltage range - 17 kV <  $V_{\rm DC}<-$  11 kV, represents the voltage range over which physically meaningful calculations can be made. Over this voltage range (-11 kV to -17 kV), the calculated remediation increases from 10 % to 90 % and agrees qualitatively with the DC only experimental data plotted in Fig. 2. For voltages above  $V_{\rm DC}=-$ 11 kV, these calculations could not converge because the ion density of the corona

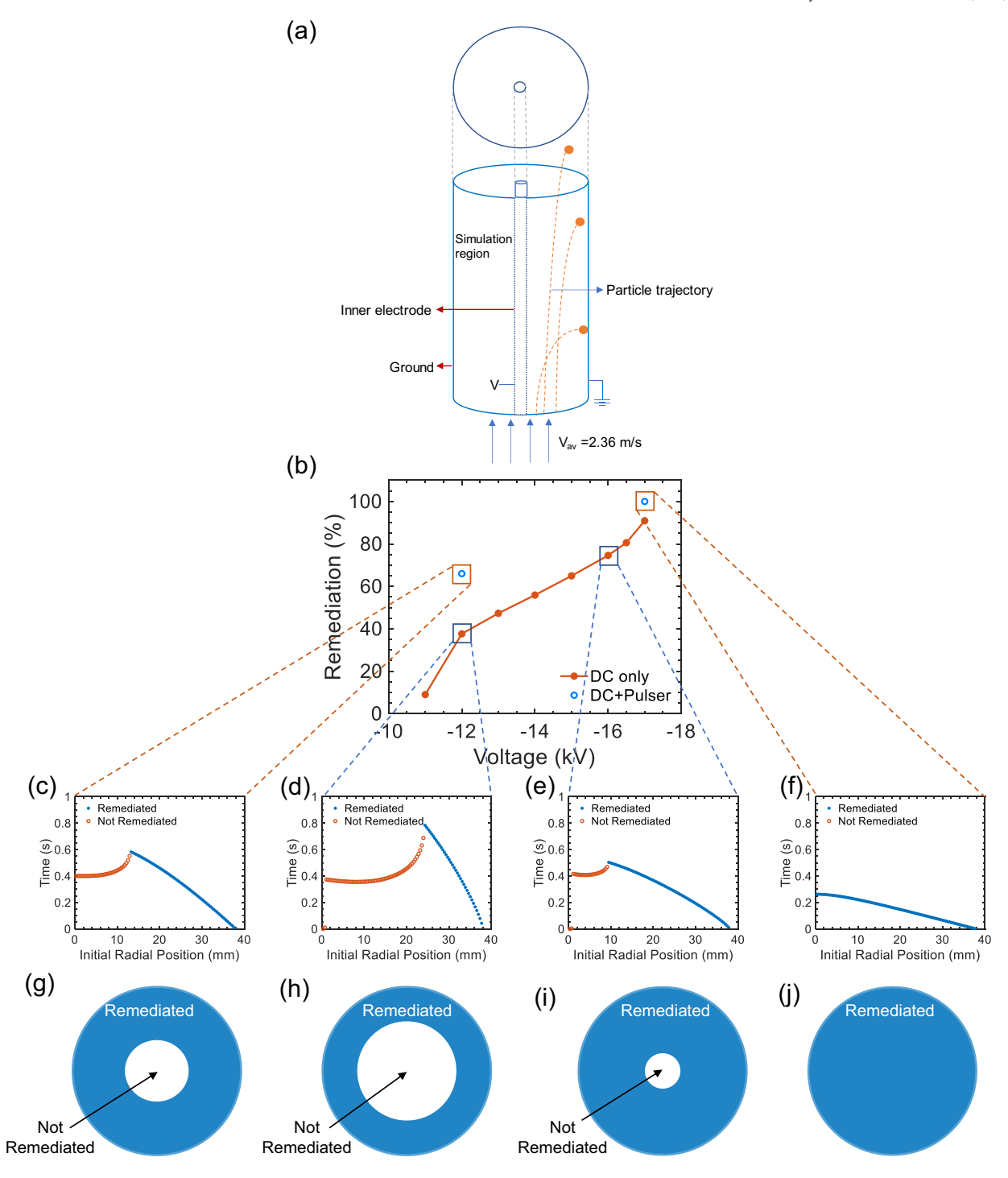


Fig. 3. (a) Schematic diagram illustrating the COMSOL simulation of the electrostatic precipitation process. (b) Calculated remediation (%) with and without high voltage nanosecond pulses plotted as a function of applied DC bias voltage. (c–f) Selected residence times of 100 nm diameter nanoparticles plotted as a function of the initial radial position and (g–j) corresponding cross-section area diagrams illustrating which regions of the reactor are remediated.

discharge was too low (i.e., theoretical upper limit). For voltages below  $V_{\rm DC}=-17~{\rm kV}$ , no experimental data could be taken because arcing occurred (i.e., experimental lower limit).

Whether or not particles are remediated depends strongly on their initial radial position, i.e., their distance from the center electrode at the entrance of the reactor, as plotted in Fig. 3c. We have plotted the residence time of a 100 nm diameter nanoparticle as a function of the initial radial position within the reactor in Fig. 3d and e. Here, we see that the nanoparticles with an initial radial position that is close to the outer cylindrical

electrode are remediated (blue data points), and the nanoparticles with initial radial positions close to the inner wire electrode are not remediated (orange data points). For relatively small DC voltages (e.g.,  $-12\,\rm kV$ ), the cross-sectional area that is not remediated represents a substantial fraction of the total cross-section of the reactor. Whereas, at relatively large DC voltages (e.g.,  $-16\,\rm kV$ ), the region that is not remediated represents a relatively small fraction of the total cross-section of the reactor. These remediated and non-remediated cross-sections are illustrated in Fig. 3h and i for the  $V_{\rm DC}=-12\,\rm kV$  and  $V_{\rm DC}=-16\,\rm kV$  data, respectively. Next,

we turn our attention to the mechanism of enhancement produced by the high voltage nanosecond pulses (i.e., transient plasma). As mentioned above, the plasma-based enhancement is more pronounced at smaller DC voltages (i.e., -10 kV DC) because of the increased ion density provided by the nanosecond pulsed plasma, which is highly effective in charging the nanoparticles (i.e., Step 4 in the simulation). With the additional charge, these nanoparticles are swept out more efficiently than those that were charged by the DC corona alone (i.e., charge-limited remediation). The open symbols in Fig. 3b show the calculated remediation obtained by increasing the charge per particle by  $2\times$  in our simulation. It should be noted that the current simulation did not incorporate bipolar charging. This results in an increase in the remediation percentage similar to that obtained experimentally by adding the high voltage nanosecond pulses in conjunction with the negative DC bias voltage. In particular, we observed a large increase in remediation at small DC bias voltages (i.e., -10 kV) and relatively small increase at large voltages (i.e. -17 kV DC). Again, at  $V_{DC} = -17$  kV, the ion density produced by the DC corona is already very high and, therefore, not much gain can be added by the transient nanosecond plasma. However, the remediation time is greatly reduced and ultimately, this will enable shorter (i.e., more compact) ESPs to be made with high remediation efficiency.

It is worth pointing out that, in these steady-state COMSOL simulations, there is no rigorous way to treat the transient ion densities produced by the nanosecond high voltage pulses. In this steady-state approach, the electrostatic Poison's equation is solved iteratively in a self-consistent fashion (Step 2), based on the steady-state ion concentrations calculated in Step 1, which includes positive ions, negative ions, and free electrons. While these steady-state ion concentrations can be calculated relatively easily for the case of a corona discharge, it is not possible to do this with streamer discharge, which is inherently stochastic and highly non-uniform. As such, there is no way of adding these time-dependent ion densities within the steady-state approach. Nevertheless, these calculations provide insight into the basic mechanism of enhancement provided by the PE-ESP approach.

The work presented here represents a proof-of-principle study of what can be achieved using the PE-ESP approach, reducing the size of the device substantially with higher efficiency compared to that of conventional ESPs. However, further development will be needed in order to solve technical issues associated with reactor cleanout and maintenance in order to be implemented in mobile source emission control systems. Though demonstrated on a relatively small system, this PE-ESP approach is scalable, unlike DPFs. One strategy for scaling up is to increase the electrostatics to a 6"-diameter reactor and then create an array of parallel reactors up to 225 (i.e.,  $15 \times 15$ ) reactors. This would correspond to a cross-sectional area of 56 ft², which is typical of the stack in an ocean-going vessel.

# 4. Conclusion

In conclusion, we have observed plasma-enhanced electrostatic precipitation (PE-ESP) of diesel engine exhaust using filter-based measurements, scanning mobility particle sizer (SMPS) measurements, and optical detection (Brewster's angle detection sensor). Here, plasma enhancement is achieved using positive high voltage nanosecond pulse discharges in conjunction with negative DC voltages. Remediation values up to 95 %are observed. With plasma enhancement, high remediation values are observed over a wide range of DC applied voltages, making this approach more robust, thus, mitigating problems associated with arcing. As such, this nanosecond transient pulsed plasma approach provides a method for eliminating instabilities in the electrostatic precipitation process. A computational model of the electrostatic precipitation process is presented, which agrees qualitatively with the DC-only experimental electrostatic precipitation data. By introducing an enhanced charge per particle, this model predicts substantial increases in the remediation efficiency similar to those observed experimentally with the application of the nanosecond high voltage pulsed plasma, thus, providing a theoretical basis for the charge-based mechanism of enhancement provided by the transient pulsed plasma. In

addition, these simulations provide physical insights into the particle trajectories and remediation times, which are greatly reduced with the plasma/charge enhancement. These reduced remediation times can ultimately enable shorter (i.e., more compact) electrostatic precipitators to be made with high remediation efficiency.

### CRediT authorship contribution statement

**Boxin Zhang:** Conceptualization, Methodology, Validation, Formal analysis, Investigation, Data Curation, Writing - Review & Editing, Visualization

Indu Aravind: Conceptualization, Methodology, Validation, Formal analysis, Investigation, Data Curation, Writing - Review & Editing, Visualization

Sisi Yang: Methodology, Validation, Data Curation

**Sizhe Weng:** Data Curation **Bofan Zhao:** Data Curation

Christi Schroeder: Methodology, Validation, Data Curation William Schroeder: Methodology, Validation, Data Curation

Mark Thomas: Data Curation Ryan Umstattd: Data Curation Dan Singleton: Data Curation Jason Sanders: Data Curation

Heejung Jung: Writing - Review & Editing, Supervision

**Stephen B. Cronin**: Conceptualization, Methodology, Validation, Formal analysis, Investigation, Data Curation, Writing - Original Draft, Writing - Review & Editing, Supervision, Project administration, Funding acquisition

## Data availability

Data will be made available on request.

# Declaration of competing interest

The authors declare that they have no known competing financial interests or personal relationships that could have appeared to influence the work reported in this paper.

# Acknowledgements

This research was supported by the Air Force Office of Scientific Research (AFOSR) grant no. FA9550-19-1-0115 (S.Y.), Army Research Office (ARO) award no. W911NF-19-1-0257 (B.Z.), National Science Foundation (NSF) award nos. CBET-2112898 (I.A.) and CHE-1954834 (B.Z.), and the James H. Zumberge Faculty Research and Innovation Fund (S.W.). This report was prepared as a result of work sponsored, paid for, in part, by the South Coast air quality management District (SCAQMD). This study was partially funded by a grant from the National Center for Sustainable Transportation (NCST), supported by U.S. Department of Transportation's University Transportation Centers Program.

# Disclaimer

The opinions, findings, conclusions, and recommendations are those of the author and not necessarily represent the views of SCAQMD. SCAQMD, its officers, employees, contracts, and subcontractors make no warranty, expressed or implied, and assume no legal liability for the information in this report. SCAQMD has not approved or disapproved this report, nor has SCAQMD passed upon the accuracy or adequacy of the information contained herein. The contents of this report reflect the views of the authors, who are responsible for the facts and the accuracy of the information presented herein. This document is disseminated in the interest of information exchange. The U.S. Government and the State of California assumes no liability for the contents or use thereof. Nor does the content necessarily reflect the official views or policies of the U.S. Government

and the State of California. This report does not constitute a standard, specification, or regulation. This report does not constitute an endorsement by the California Department of Transportation (Caltrans) of any product described herein.

#### Appendix A. Supplementary data

Supplementary data to this article can be found online at https://doi.org/10.1016/j.scitotenv.2022.158181.

#### References

- Babaeva, N.Y., Naidis, G.V., 2016. Modeling of streamer dynamics in atmospheric-pressure air: influence of rise time of applied voltage pulse on streamer parameters. IEEE Trans. Plasma Sci. 44 (6), 899–902.
- Bidoggia, B., et al., 2020. Reduction of dust emission by coromax micro-pulse power supplies at an oil shale fired power plant. J. Electrost. 105, 103447.
- Brown, D.M., et al., 2001. Size-dependent proinflammatory effects of ultrafine polystyrene particles: a role for surface area and oxidative stress in the enhanced activity of ultrafines. Toxicol. Appl. Pharmacol. 175 (3), 191–199.
- Burtscher, H., 2005. Physical characterization of particulate emissions from diesel engines: a review. J. Aerosol Sci. 36 (7), 896–932.
- Chow, J.C., et al., 2006. Health effects of fine particulate air pollution: lines that connect. J. Air Waste Manage. Assoc. 56 (10), 1368–1380.
- Code of Federal Regulations (CFR) Title 40 Protection of Environment, 2022. Chapter I ENVIRONMENTAL PROTECTION AGENCY, Subchapter U AIR POLLUTION CONTROLS, Part 1065 ENGINE-TESTING PROCEDURES.
- Dockery, D., et al., 1993. An association between air pollution and mortality in six U.SCities. N. Engl. J. Med. 329 (24), 1753–1759.
- Fushimi, C., et al., 2008. Influence of polarity and rise time of pulse voltage waveforms on diesel particulate matter removal using an uneven dielectric barrier discharge reactor. Plasma Chem. Plasma Process. 28 (4), 511–522.
- Grass, N., Hartmann, W., Romheld, M., 2001. Microsecond pulsed power supply for electrostatic precipitators. Conference Record of the 2001 IEEE Industry Applications Conference. 36th IAS Annual Meeting (Cat. No.01CH37248).
- Grass, N., Hartmann, W., Klockner, M., 2004. Application of different types of high-voltage supplies on industrial electrostatic precipitators. IEEE Trans. Ind. Appl. 40 (6), 1513–1520.
- Hall, H.J., 1990. History of pulse energization in electrostatic precipitation. J. Electrost. 25
- Hayashi, H., 2011. Collection of Diesel Exhaust Particle Using Electrostatic Charging Prior to DPF and Regeneration of DPF Using Sliding Discharge.
- Hayashi, H., et al., 2009. Electrostatic charging and precipitation of diesel soot. 2009 IEEE Industry Applications Society Annual Meeting.
- Huiskamp, T., et al., 2017. Spatiotemporally resolved imaging of streamer discharges in air generated in a wire-cylinder reactor with (sub)nanosecond voltage pulses. Plasma Sources Sci. Technol. 26 (7), 075009.
- IARC, 2012. IARC: DIESEL ENGINE EXHAUST CARCINOGENIC [Press Release]. World Health Organization.
- Jamriska, M., et al., 2004. Diesel bus emissions measured in a tunnel study. Environ. Sci. Technol. 38 (24), 6701–6709.
- Khan, M.Y., et al., 2012. Characterization of PM-PEMS for in-use measurements conducted during validation testing for the PM-PEMS measurement allowance program. Atmos. Environ. 55, 311–318.
- Kim, K., Kim, T., 2019. Nanofabrication by thermal plasma jets: from nanoparticles to low-dimensional nanomaterials. J. Appl. Phys. 125 (7), 070901.
- Kim, H.J., et al., 2013. Collection performance of an electrostatic filtration system combined with a metallic flow-through filter for ultrafine diesel particulate matters. Int. J. Automot. Technol. 14 (3), 489–497.
- Kim, H.J., et al., 2015. Submicrometer PM removal of an ESP combined with a metallic foam filter for large volumetric diesel engines. IEEE Trans. Ind. Appl. 51 (5), 4173–4179.
- Kittelson, D.B., Pui, D.Y., Moon, K., 1986. Electrostatic collection of diesel particles. SAE Trans. 51–62.
- Kuwahara, T., et al., 2020. Pilot-scale combined reduction of accumulated particulate matter and NOx using nonthermal plasma for marine diesel engine. IEEE Trans. Ind. Appl. 56 (2), 1804–1814.
- Lawless, P.A., Altman, R.F., 1994. ESPM: an advanced electrostatic precipitator model. Proceedings of 1994 IEEE Industry Applications Society Annual Meeting, IEEE.
- Lawless, P.A., Sparks, L.E., 1988. Modeling particulate charging in ESPs. IEEE Trans. Ind. Appl. 24 (5), 922–927.

- Lighty, J.S., Veranth, J.M., Sarofim, A.F., 2000. Combustion aerosols: factors governing their size and composition and implications to human health. J. Air Waste Manage. Assoc. 50 (9), 1565–1618.
- Moosmüller, H., et al., 2001. Time resolved characterization of diesel particulate emissions. 1.

  Instruments for particle mass measurements. Environ. Sci. Technol. 35 (4), 781–787.
- Mun, M.K., et al., 2020. Direct nanoparticle coating using atmospheric plasma jet. J. Nanopart. Res. 22 (6), 1–11.
- Oberdörster, G., et al., 2004. Translocation of inhaled ultrafine particles to the brain. Inhal. Toxicol. 16 (6–7), 437–445.
- Oberdörster, G., Oberdörster, E., Oberdörster, J., 2005. Nanotoxicology: an emerging discipline evolving from studies of ultrafine particles. Environ. Health Perspect. 113 (7), 823–839
- Okubo, M., et al., 2010. Single-stage simultaneous reduction of diesel particulate and NOx using oxygen-lean nonthermal plasma application. IEEE Trans. Ind. Appl. 46 (6), 2143–2150.
- Okubo, M., et al., 2017. Simultaneous reduction of diesel particulate and NOx using a catalysis-combined nonthermal plasma reactor. IEEE Trans. Ind. Appl. 53 (6), 5875-5882.
- Panel, H.D.E., 2015. Diesel Emissions and Lung Cancer: An Evaluation of Recent Epidemiological Evidence for Quantitative Risk Assessment. Health Effects Institute, Boston, MA.
- Particle Tracing Module User's Guide https://doc.comsol.com/5.6/doc/com.comsol.help.particle/ParticleTracingModuleUsersGuide.pdf.
- Pope III, C.A., et al., 2002. Lung cancer, cardiopulmonary mortality, and long-term exposure to fine particulate air pollution. JAMA: The Journal of the American Medical Association 287 (9), 1132–1141.
- Ris, C., 2007. US EPA health assessment for diesel engine exhaust: a review. Inhal. Toxicol. 19 (sup1), 229–239.
- Ristovski, Z.D., et al., 2012. Respiratory health effects of diesel particulate matter. Respirology 17 (2). 201–212.
- Rubinetti, D., Weiss, D.A., Egli, W., 2015. Electrostatic precipitators–modelling and analytical verification concept. University of Applied Sciences Northwestern Switzerland, Windisch, Switzerland, COMSOL CONFERENCE.
- Saiyasitpanich, P., et al., 2007. Removal of diesel particulate matter (DPM) in a tubular wet electrostatic precipitator. J. Electrost. 65 (10), 618–624.
- Samet, J.M., et al., 2000. Fine particulate air pollution and mortality in 20 U.S. cities, 1987–1994. N. Engl. J. Med. 343 (24), 1742–1749.
- Schauer, J.J., Kleeman, M.J., Cass, G.R., 1999. Measurement of emissions from air pollution sources. 2:  $C_1$  through  $C_{30}$  organic compounds from medium duty diesel trucks. Environ. Sci. Technol. 33 (10), 1578–1587.
- Silvestre de Ferron, A., et al., 2008. Removal of diesel soot particules using an esp supplied by a hybrid voltage. Eur. Phys. J. Appl. Phys. 43 (1), 103–109.
- Song, C.-L., et al., 2009. Simultaneous removals of NOx, HC and PM from diesel exhaust emissions by dielectric barrier discharges. J. Hazard. Mater. 166 (1), 523–530.
- Sudrajad, A., Yusof, A.F., 2015. Review of electrostatic precipitator device for reduce of diesel engine particulate matter. Energy Procedia 68 (C), 370–380.
- Takasaki, M., et al., 2015. Electrostatic precipitation of diesel PM at reduced gas temperature. 2015 IEEE Industry Applications Society Annual Meeting.
- Teunissen, J., Sun, A., Ebert, U., 2014. A time scale for electrical screening in pulsed gas discharges. J. Phys. D. Appl. Phys. 47 (36), 365203.
- The Plasma Module User's Guide https://doc.comsol.com/5.3/doc/com.comsol.help.plasma/PlasmaModuleUsersGuide.pdf.
- Turan, N., et al., 2021. Atmospheric pressure and ambient temperature plasma jet sintering of aerosol jet printed silver nanoparticles. ACS Appl. Mater. Interfaces 13 (39), 47244–47251.
- Vinh, T.Q., et al., 2012. Effects of particulate matter on NOx removal in dielectric barrier discharges. J. Energy Inst. 85 (3), 163–169.
- Wang, J.J., et al., 2019. Numerical model of the Mars electrostatic precipitator. COMSOL Conference 2019.
- Winands, G.J.J., et al., 2008. Analysis of streamer properties in air as function of pulse and reactor parameters by ICCD photography. J. Phys. D. Appl. Phys. 41 (23), 234001.
- Won-Ho, K., et al., 1999. A high voltage pulsed power system for electrostatic precipitators. Conference Record of the 1999 IEEE Industry Applications Conference. Thirty-Forth IAS Annual Meeting (Cat. No.99CH36370).
- Yang, S., et al., 2021. Plasma-enhanced electrostatic precipitation of diesel exhaust using high voltage nanosecond pulse discharge. J. Environ. Chem. Eng. 9 (6), 106565.
- Yang, S., et al., 2021. Transient plasma-enhanced remediation of nanoscale particulate matter in restaurant smoke emissions via electrostatic precipitation. Particuology 55, 43–47.
- Zukeran, A., Ninomiya, K., 2013. SOx and PM Removal Using Electrostatic Precipitator With Heat Exchanger for Marine Diesel.
- Zukeran, A., Sawano, H., Yasumoto, K., 2019. Collection characteristic of nanoparticles emitted from a diesel engine with residual fuel oil and light fuel oil in an electrostatic precipitator. Energies 12 (17), 3321.